

New, best-in-class 900-A 1200-V EconoDUAL™ 3 with IGBT 7: highest power density and performance

Klaus Vogel, Jan Baurichter, Oliver Lenze, Ulrich Nolten, Alexander Philippou, Philipp Ross, Andreas Schmal, Christoph Urban

Corresponding author: Klaus Vogel, klaus.vogel@infineon.com

Infineon Technologies AG, Germany

Abstract

The development of the new semiconductor generation targets current density increase with the aim to reduce system costs for inverter manufacturers. It is crucial to implement the new technology in a given module footprint to facilitate the upgrade of existing inverter systems. This approach leads to a fast market penetration. The switching characteristics of the improved IGBTs and diodes have to fit the characteristics of the selected module housing. This is true, especially with regard to oscillation behavior, since the module current is higher, and the reduction of module stray inductance is limited. At the same time, improving the housing is an important consideration to be able to handle higher currents and temperatures. For the user of the new device, the benefits are clear: higher inverter output current for the same frame size, and avoidance of paralleling of IGBT modules. Both possibilities lead to the simplification of the inverter systems and to lower costs. In this paper, all the technical aspects of the new EconoDUAL™ 3 with TRENCHSTOP™ IGBT 7 medium-power and corresponding emitter-controlled 7 diode for general-purpose drives application will be discussed.

1 Target application

One target application for the new IGBT 7 generation is the general-purpose drive (GPD) application in a power range above 90 kW. It is important to take into consideration the typical application parameters to understand the improvement levers to achieve a benefit compared to the predecessor IGBT 4 technology.

Typically switching frequencies for GPDs in the power range above 90 kW are in the range of 2 to 2.5 kHz [1,2]. Most inverter manufacturers use advanced modulation methods such as discontinuous pulse width modulation (DPWM) [3] that leads to a reduction of switching losses by half compared to traditional continuous modulation [4].

For the IGBT 7 development and for the following study, a switching frequency of 1 kHz and 2.5 kHz, both as continuous PWM, are selected to evaluate the new technology. The results are thus valid for higher switching frequencies using DPWM.

Furthermore, a characteristic of this application is the use of an air-cooled heatsink of extruded aluminum at a maximum ambient temperature of 40°C.

The nominal current of the GPD inverter is dimensioned taking into account normal and heavy-duty overload pulses at different overload

current levels. Therefore, the maximum allowed IGBT operation temperature has to also consider this type of operation.

Finally, the maximum steepness of the voltage slope ($du/dt_{10-90\%}$) during IGBT turn-on and turn-off is typically limited to maximum 5 kV/ μ s due to motor windings lifetime and drive shaft corrosion [5] as well as for electromagnetic compatibility (EMC).

A simulation using all the above-mentioned application parameters is implemented with the FF60012ME4_B72 and the results are shown in Fig. 1.

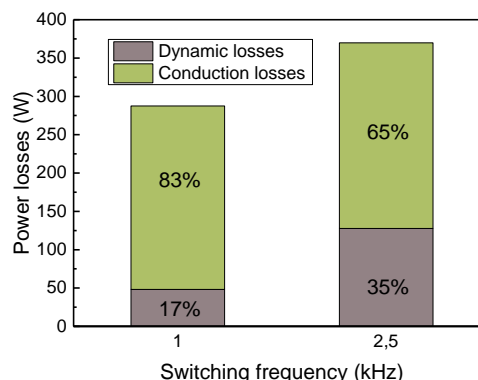


Fig. 1: Loss distribution FF60012ME4_B72 at 350 A and typical GPD conditions for this power class.

It becomes visible that the conduction losses of the IGBT and diode predominate over the dynamic losses. At 1 kHz these losses represent 83% and at 2.5 kHz 65% of all semiconductor losses. This, together with the fact that the switching speed for electrical-motor-related applications cannot be increased above 5 kV/μs, leads to the conclusion that the main lever for device optimization is the static loss reduction.

In the next chapter, the details of the new technology improvement based on the technical background mentioned above will be presented.

2 1200-V TRENCHSTOP™ IGBT 7 medium-power technology

2.1 Basics

While the recently presented 1200-V TRENCHSTOP™ IGBT 7 low-power technology has been optimized for products with nominal currents up to 200 A [6], this paper focuses on the new TRENCHSTOP™ IGBT 7 medium-power technology. This chip has been optimized for the use in EconoDUAL™ 3 modules with nominal currents up to 900 A, which means a current increase of 50% with respect to the previous best-in-class EconoDUAL™ 3 FF600R12ME4_B72 with 600 A. For this purpose, optimizations regarding thickness and backside processes were carried out to obtain a soft-switching device with reduced conduction losses, similar dynamic losses compared to IGBT 4, while maintaining sufficient short-circuit ruggedness. This is enabled by the micro-pattern trench (MPT) structure, presented in Fig. 2.

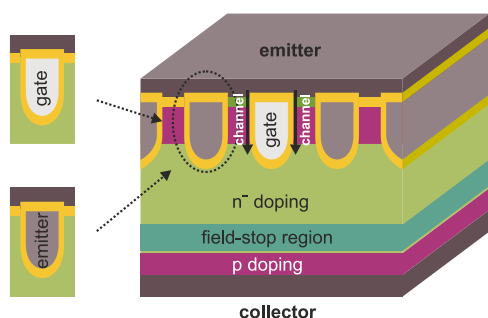


Fig. 2: Micro-pattern trench cell with an active channel in the center and indicated options of gate trenches with inactive mesa and emitter trenches [6].

By using narrow parallel trenches, which are separated by sub-micron mesas with active gate trenches, gate trenches with inactive mesa and emitter trenches, MPT-IGBTs allow for optimization of the contact scheme, to achieve

both fast carrier removal during switching and a reduced voltage drop across the drift region [7].

2.2 Static losses

The corresponding normalized output characteristics of the IGBT 7 MPT technology and the IGBT 4 are presented in Fig. 3 for room temperature, 125°C, 150°C and for the TRENCHSTOP™ IGBT 7 additionally at 175°C.

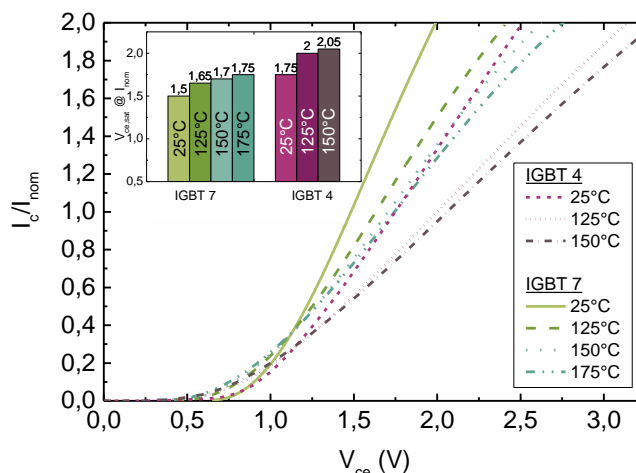


Fig. 3: Normalized output characteristics of the 1200 V TRENCHSTOP™ IGBT 4 medium power compared with the 1200 V TRENCHSTOP™ IGBT 7, measured at $V_{ge}=15$ V.

A reduction of $V_{ce,sat}$ from 2.05 V to 1.70 V by 350 mV at nominal current is observed when comparing both IGBT technologies, which demonstrates the optimization of the device.

2.3 $du/dt_{10-90\%}$ controllability

Besides the static characteristics of IGBT power modules, dynamic switching behavior also plays an important role for the overall performance. Especially for drive applications where the voltage slope is typically limited to below 5 kV/μs, as mentioned in the introduction, a controllability of the $du/dt_{10-90\%}$ as a function of the external gate resistance ($R_{g,ext}$) of the gate driver unit is mandatory. Typically during turn-on, the $du/dt_{10-90\%}$ shows its highest values at low temperatures, e.g. 25°C, and low currents, e.g. 10% of the nominal current (I_{nom}). During turn-off the highest voltage slopes are observed at high currents, e.g. $1 \cdot I_{nom}$. Fig. 4 presents the $du/dt_{10-90\%}$ during turn-on and turn-off at the above- mentioned conditions for the TRENCHSTOP™ IGBT 4 and IGBT 7.

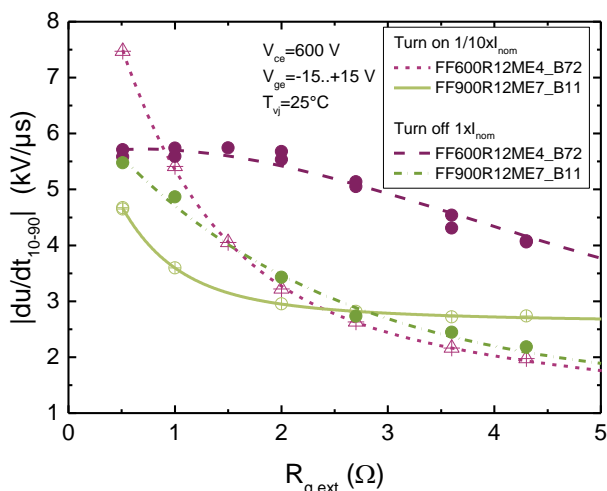


Fig. 4: Voltage slope $du/dt_{10-90\%}$ vs. $R_{g,ext}$ during turn-on and turn-off for TRENCHSTOP™ IGBT 4 and IGBT 7 in the EconoDUAL™ 3 FF600R12ME4_B72 and FF900R12ME7_B11, respectively.

In addition to the good controllability of the $du/dt_{10-90\%}$ by the external gate resistance, in particular, the controllability of the du/dt during turn-off has been improved for the seventh chip generation in contrast to the IGBT 4.

2.4 Overvoltage and softness

A significant static-loss reduction, and the increase of the IGBT maximum operation temperature $T_{vj,op}$ from 150°C (IGBT 4) to 175°C (IGBT 7), allows for higher levels of switching current per device, which in turn leads to increased rates of change of current (di/dt). To maintain the same switching speed at a higher current, the total stray inductance has to be reduced. This requirement can be summarized by the simple constraint $L_{\sigma} \cdot I = \text{constant}$ [8].

The effect of stray inductance on a power converter system has a particularly negative impact during turn-off of the IGBT.

The IGBT collector-emitter overvoltage is described by the equation $\Delta U = L_{\sigma} \cdot di/dt$, which shows it is directly proportional to the stray inductance and the rate of current change. The current shape is also dependent on the applied voltage between collector and emitter. Higher voltage applied to the IGBT during turn-off causes an earlier removal of charges from the device, and the tail current disappears [8]. This means that the parasitic inductance that causes an overvoltage, accelerates the current fall, and this again increases the overvoltage.

In addition, high di/dt and L_{σ} can lead to oscillations that cause electromagnetic interference (EMI). This is a consequence of exciting a resonant circuit

consisting of the parasitic inductance in the commutation loop and the chip capacitance.

It is possible for a system to have a level of parasitic inductance that will cause the voltage across the silicon to exceed the chip breakdown voltage, and hence, module failure. The worst-case operating conditions that cause excessive overvoltage are switching at low junction temperatures due to the faster switching of the chip, high DC bus levels, or at short-circuit and high-current overload. There are several methods commonly used to reduce these overvoltage occurrences, for example, by optimizing the gate-resistor value, adding snubber capacitors, voltage active clamp circuits, or utilizing lower switching-speed silicon. However, these methods have limitations. Snubber capacitors are expensive, and can create additional current oscillations to and from the main capacitor bank. Active clamp circuits are challenging to dimension.

Due to the requirement to increase the current capability of the EconoDUAL™ 3 housing up to 900 A, the stray inductance could not be changed significantly. Therefore, the turn-off behavior of the IGBT had to be adapted. As a result, the TRENCHSTOP™ IGBT 7 is able to turn off 900 A with a maximum overvoltage $V_{ce,max}$ similar to the IGBT 4 at turn-off of 600 A at almost identical di/dt , which is presented in Fig. 5.

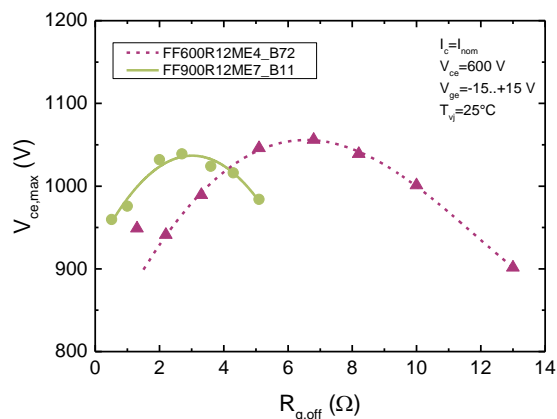


Fig. 5: Maximum overvoltage $V_{ce,max}$ at turn-off of 900 A for the TRENCHSTOP™ IGBT 7 and 600 A for the IGBT 4 as a function of the external gate resistance $R_{g,off}$.

Within this context, Fig. 6 shows the turn-off switching curves at nominal current at 25°C for the FF600R12ME4_B72 and the FF900R12ME7_B11 at external gate resistances of $R_{g,off}=6.8 \Omega$ for the 600 A module and $R_{g,off}=2.4 \Omega$ for the 900 A

module, where the highest di/dt , and therefore the highest $V_{ce,max}$, occurred.

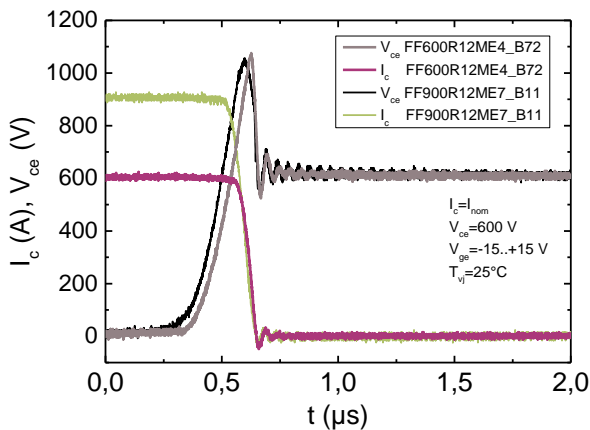


Fig. 6: Turn-off curves of the FF600R12ME4_B72 at $R_{g,off}=6.8 \Omega$ and the FF900R12ME7_B11 at $R_{g,off}=2.4 \Omega$, where the highest di/dt and therefore the highest $V_{ce,max}$ occurred.

As can be seen, a similar switching behavior is observed for the TRENCHSTOP™ IGBT 7, although a 50% higher current is turned off.

2.5 Dynamic switching

The corresponding turn-off losses (E_{off}) of the IGBT 4 in comparison to the IGBT 7 are presented in Fig. 7 as a function of the collector current I_c at different temperatures.

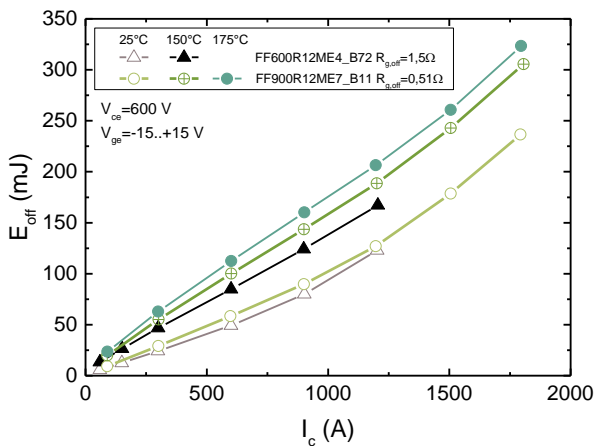


Fig. 7: Turn-off losses E_{off} of the FF600R12ME4_B72 and the FF900R12ME7_B11 as a function of the collector current I_c .

In fact, the reduction of the saturation voltage and the given device softness result in higher turn-off losses at similar collector currents. Hence, an increase of 15-20% in E_{off} is evident for the FF900R12ME7_B11 in comparison to the FF600R12ME4_B72. The chosen external gate resistances coincide with the datasheet values, which have been defined in such a way that switching without cut-off oscillations of the IGBT

and diode at 25°C is ensured. Moreover, quite similar du/dt values are present (see Fig. 3) for the FF600R12ME4_B72 and the FF900R12ME7_B11 at those gate resistances for turn-on as well as for turn-off.

In contrast to E_{off} , the turn-on losses (E_{on}) of the 900-A IGBT 7 module are lower than those of the 600-A IGBT 4 module when a similar collector current is turned on, which is presented in Fig. 8 for both chip technologies.

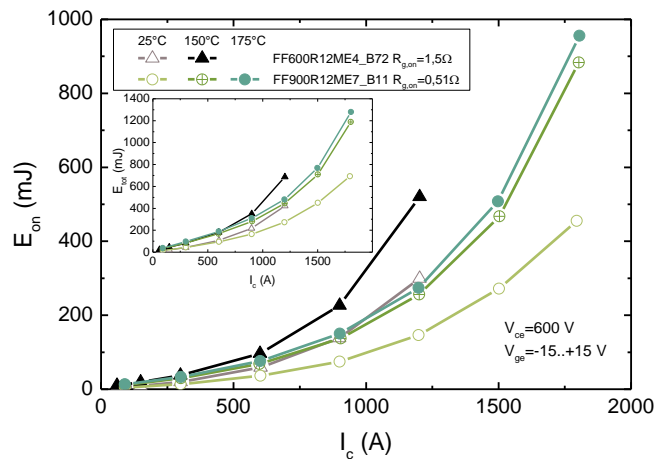


Fig. 8: Turn-on losses E_{on} of the FF600R12ME4_B72 and the FF900R12ME7_B11 as a function of the collector current I_c . The insert shows E_{tot} , the sum of E_{on} and E_{off} .

As a result, the total IGBT losses (E_{tot}) which are the sum of E_{on} and E_{off} remain nearly the same (insert in Fig. 8). Especially, below 600 A, both modules show identical losses. For completion, Fig. 9 shows typical turn-on switching curves of the FF900R12ME7_B11 at a collector current of 900 A for temperatures of 25°C and 175°C.

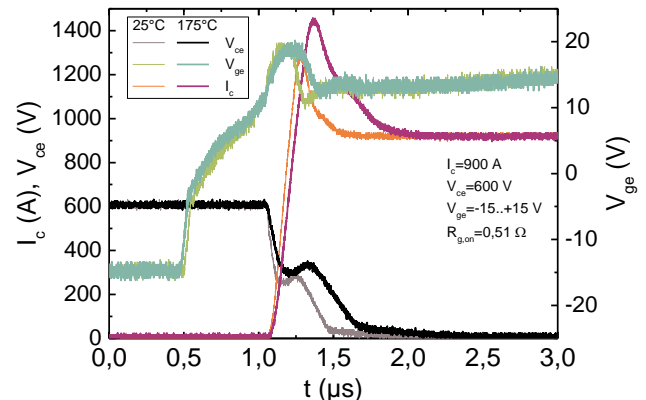


Fig. 9: Turn-on switching curve of the EconoDUAL™ 3 FF900R12ME7_B11 at 25°C and 175°C.

As expected, the increase of the temperature results in a decrease of the current slope (di/dt) and therefore, in a reduced inductive voltage drop. Moreover, the increase in the recovery charge of

the diode with higher temperature is visible by an increased reverse-recovery peak. More details of the emitter-controlled 7 diode are presented in the next section.

The cell concept of the IGBT 7 enables a sufficient short-circuit capability for standard drives applications, i.e. a short-circuit pulse length of more than 8 μs is possible at 150°C, whereas a short-circuit withstand-time of more than 6 μs is possible at 175°C.

3 1200-V emitter-controlled 7 medium power technology

On the one hand, an improvement of the IGBT performance is mandatory to increase the current capability of new power modules. However, the IGBT optimization alone is not sufficient. Also the freewheeling diode has to be improved to achieve the highest power gain. Therefore, the diode is optimized in such a way that an adequate softness during diode recovery is achieved while maintaining low losses. In contrast to the turn-off behavior of an IGBT, the diode softness is most critical at low currents, e.g. $0,1 \cdot I_{\text{nom}}$. Corresponding switching curves of the diode recovery phase at 25°C are presented in Fig. 10 for the emitter-controlled HE in the FF600R12ME4_B72 and the emitter-controlled 7 diode in the FF900R12ME7_B11.

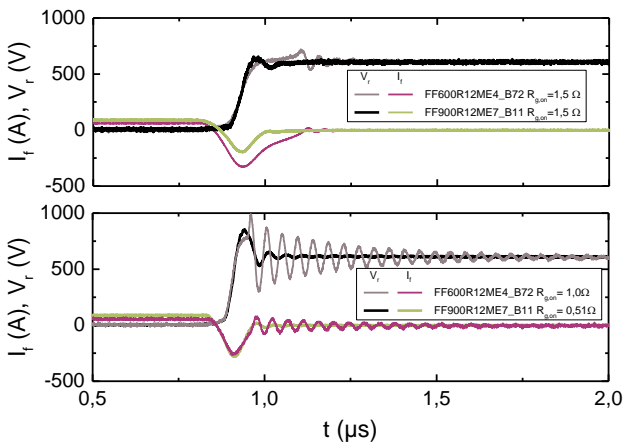


Fig. 10: Switching curves of the emitter-controlled HE in the FF600R12ME4_B72 and the emitter-controlled 7 diode in the FF900R12ME7_B11

It clearly becomes visible that the emitter-controlled HE diode cannot be used at an external gate resistance lower than 1.5 Ω . Here, a diode snap-off occurs at lower $R_{g,on}$ values such as 1.0 Ω as presented in the bottom graph, whereas the emitter-controlled 7 diode can be used even at $R_{g,on}=0.51 \Omega$ without showing any softness issues.

Regarding the recovery losses (E_{rec}) of the diodes in Fig. 11, the emitter-controlled 7 diode shows nearly the same E_{rec} as the emitter-controlled HE, although the di/dt is 26% to 31% higher than for the emitter-controlled HE.

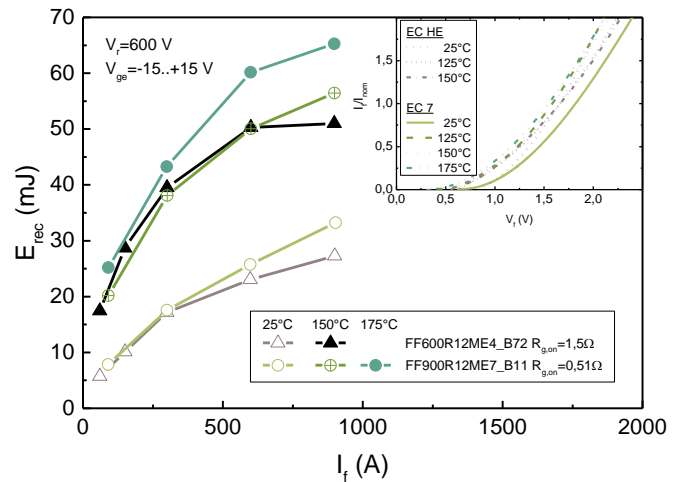


Fig. 11: Diode recovery losses as a function of the forward current for FF600R12ME4_B72 and FF900R12ME7_B11 module at different temperatures. The insert shows the normalized forward characteristics.

To complete this section, the forward characteristics of the diodes are presented in the insert of Fig. 11.

4 Module housing and junction temperature specification

4.1 Module housing adaptation

The new chipset will lead to 50% higher nominal current compared to the former generation. Therefore, some adaptation of the housing is necessary to carry the higher current, in particular, improvement of the main terminals. For this, a new housing was developed and the internal module design changed in a way that improves the current capability of the main terminals.

4.2 IGBT and FWD junction temperature specification

While the IGBT 4 has a specified absolute maximum temperature of $T_{vj,op}$ equal to 150°C, without differentiation between continuous and overload operation, the IGBT 7 will be specified

taking into account the GDP application requirement described in Chapter 1 and in [9].

Fig. 12 depicts the IGBT 7 and EC 7 junction-temperature specification.

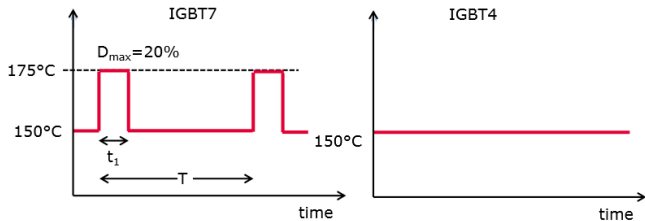


Fig. 12: IGBT 7 (left side) compared to the IGBT 4 (right side) virtual junction temperature specification. The overload duration where the IGBT 7 $T_{vj,op}$ is above 150°C must be within 20% of the load cycle time (T), e.g. $t_1 = 60s$ every $T = 300s$.

The IGBT 7 $T_{vj,op}$ specification is made taking into account the typical overload scenarios specified by the drives manufacturers, and can cover the 3 seconds as well as the 60 seconds overload pulses. The impact in the application will be presented in the next chapters.

5 Application tests and results

All the characteristics of the newly developed FF900R12ME7_B11 described above will lead to an improvement in performance compared to the FF600R12ME4_B72 device. To evaluate and compare the performance of these two devices, a series of application tests was performed and the temperatures evaluated with an infrared camera.

The test parameters were set taking into account the information described in Chapter 1 and listed in Table 1:

Topology	H-Bridge
Heatsink	Air cooled heatsink
Switching frequency	1 and 2.5 kHz
Modulation Method	Continuous PWM
Gate-Emitter Voltage	-8 V to +15 V
DC-Link Voltage	621 V
Modulation Index	0.95
cos phi	0.9
du/dt _{10-90%}	< 5kV/μs
IR-Camera Picture Rate	30 pictures per Second
Ambient Temperature	20 °C* (40°C)

Table 1: Typical GDP parameters used to compare IGBT 7 with IGBT 4 in the application. *The required ambient temperature of 40°C cannot be adjusted with the test setup.

The test setup is depicted in Fig. 13.

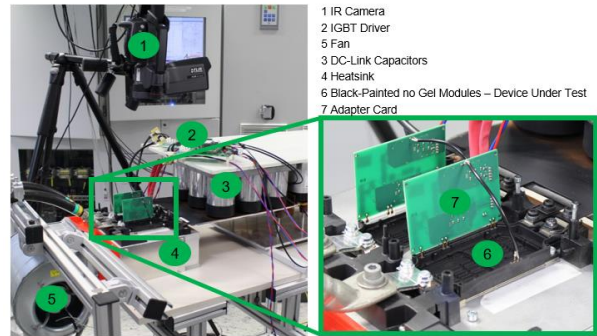


Fig. 13: Photography of the test setup. The test conditions are described in Table 1.

5.1 FF600R12ME4_B72 vs. FF900R12ME7_B11 – Output current and temperature reduction

The results of the experiment are visualized in Fig. 14 and Fig. 15.

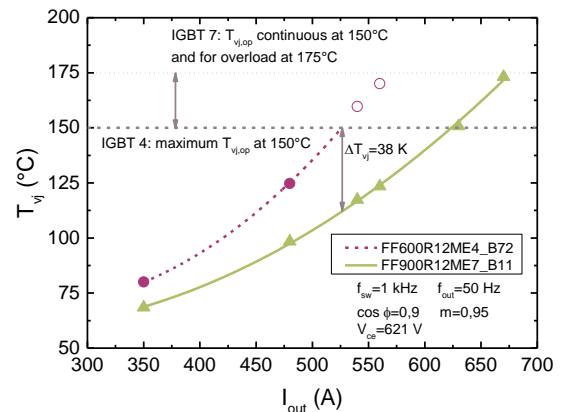


Fig. 14: IGBT junction temperature as a function of output current at 1 kHz and conditions described in Table 1.

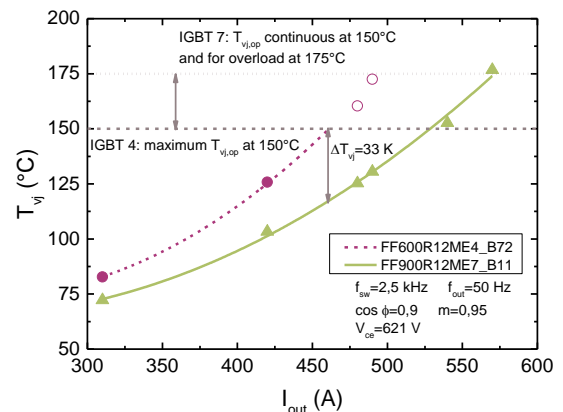


Fig. 15: IGBT junction temperature as a function of output current at 2.5 kHz and conditions described in Table 1.

It becomes visible that at 1 kHz continuous PWM and the same output current, the module using the IGBT 7 technology operates at 38 K lower temperature compared to the IGBT 4 device. Pushing the new module to the limit of the specified temperature leads to 150 A higher output current. At 150°C the IGBT 7 still has a benefit of 95 A more compared with the IGBT 4.

Also at 2.5 kHz continuous PWM modulation, the benefit of the new technology is significant: 33 K lower temperature at the same current and 70 A at 150°C and 110 A at 175°C more maximum output current are possible.

5.2 FF600R12ME4_B72 vs. FF900R12ME7_B11 – DC-terminal temperature reduction

Figure 16 illustrates the temperature reduction achieved using the new housing of the FF900R12ME7_B11 compared with the FF600R12ME4_B72.

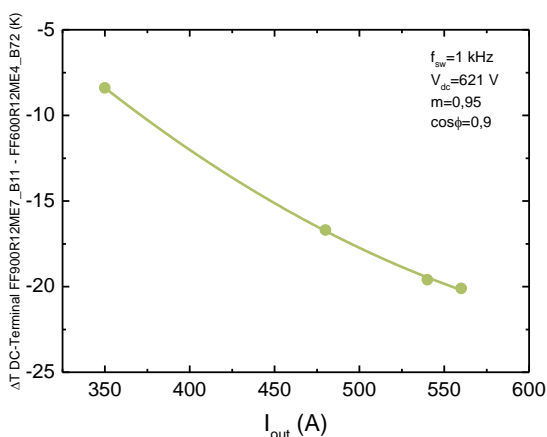


Fig. 16: Temperature improvement comparing the DC-busbar temperature of the new and former housing.

The new housing of the FF900R12ME7_B11 module leads to a temperature reduction of up to 20 K on the DC-busbar compared to the FF600R12ME4_B72 at the same output current.

In Figure 17 two infrared pictures, showing the temperature distribution of the two modules at identical application conditions, can be compared.

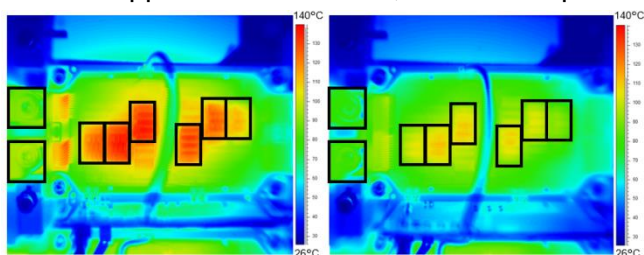


Fig. 17: FF600R12ME4_B72 (left side) and FF900R12ME7_B11 (right side), both operating at the

same conditions at 420 A and 2.5 kHz. Same temperature scale. Parts of the inverter evaluated regarding temperature black framed.

This comparison makes the lower temperature of the different components in the system visible using the FF900R12ME7_B11 instead of the FF600R12ME4_B72 module. Mainly IGBTs, FWDs, DCBs, module terminals, DC-link busbar terminals and bond wires are operating at lower temperature with the new device.

5.3 FF600R12ME4_B72 vs. FF900R12ME7_B11 – GPD frame size

In this part of the test, the parameters regarding output current for normal duty (ND) and heavy duty (HD) of a GPD manufacturer [1] were selected to evaluate the maximum possible frame size current for the different technologies. The parameters are listed in Table 2.

	Frame size 370 A	Frame size 477 A
Rated Current I_{ND}	370	477
Normal Duty 60s $1.1 \times I_{ND}$	407	525
Normal Duty 3s $1.5 \times I_{ND}$	555	716
Rated Current (I_{HD})	312	370
Heavy Duty 60s $1.5 \times I_{HD}$	468	555
Heavy Duty 3s $2 \times I_{HD}$	624	740

Table 2: Selected parameter to test the framesize capability of the two modules.

The rated output current was applied on the semiconductor at the conditions described in Table 1 and at 2.5 kHz. The temperature of the entire system was in steady state before overload current application. The thermal behavior of the system is shown in Fig. 18 and 19.

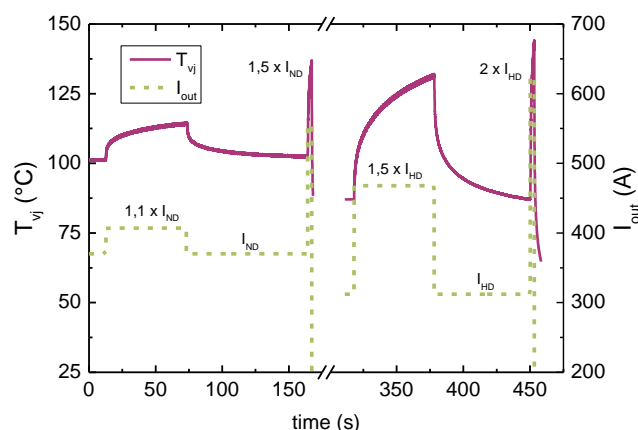


Fig. 18: Frame size 370 A, FF600R12ME4_B72 device: Measurement results at rated current ND and HD, normal-duty and heavy-duty overload pulses.

The IGBT 4 solution is on the temperature limit at frame size 370 A. During the 3 seconds heavy-duty overload pulse the IGBT T_{vj} achieves a value of 142°C.

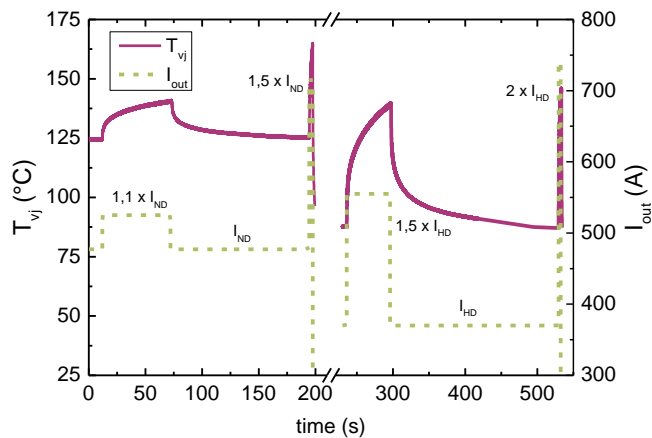


Fig. 19: Frame size 477 A, FF900R12ME7_B11 device: Measurement results at rated current ND and HD, normal-duty and heavy-duty overload pulses.

The IGBT 7 device is able to fulfill the requirement of frame size 477 A. During all needed current levels the FF900R12ME7_B11 is still inside the IGBT 7 specification presented in Fig. 12. Since the ambient temperature in the test was 20°C instead of the required 40°C, the achieved results are valid for the purpose of comparison. Hence, inverter manufacturers can achieve the same output current at 40°C by using an improved heatsink, using discontinuous PWM, and/or reducing the switching frequency.

6 Summary

The newly developed chipset of IGBT 7 and emitter-controlled 7 diode is user-friendly and optimized to fulfill the general purpose drives (GPD) requirements. A significant reduction of static losses, good controllability, sufficient softness at all application-relevant current levels, and high short-circuit capability has been achieved. This, together with the improvement in the EconoDUAL™ 3 housing and the new temperature specifications for covering the drives overload requirement, leads to a high degree of freedom for the inverter design engineer.

The conducted application tests impressively demonstrate the improved performance as compared to the former generation. The new FF900R12ME7_B11 achieves 38 K lower temperature compared to the FF600R12ME4_B72 module at the same current. Alternatively, up to 150 A higher output current can be achieved.

Taking into account the typical GPD normal-duty and heavy-duty design criteria, a frame size jump from 370 A to 477 A is possible with the EconoDUAL™ 3 housing using IGBT 7 instead of IGBT 4.

7 References

- [1] WEG-cfw11-users-manual-400v-sizes-f-g-and-h-10000784107
<https://static.weg.net/medias/downloadcenter/ha4/h8a/WEG-cfw11-users-manual-400v-sizes-f-g-and-h-10000784107-en.pdf>
- [2] SINAMICS G120, Power Module PM240, Hardware Installation Manual · 072009, Page 65
- [3] M. Depenbrock: Pulse width control of a 3-phase inverter with nonsinusoidal phase voltages in Conf. Rec. IEEE Int. Semiconductor Power Conversion Conf., 1977, pp. 399–403.
- [4] M. Bierhoff, et al., An Analysis on Switching Loss Optimized PWM Strategies for Three Phase PWM Voltage Source Converters, The 33rd Annual Conference of the IEEE Industrial Electronics Society (IECON), Nov. 5-8, 20
- [5] K. Vogel, et al., Improve the efficiency in AC-Drives: New Semiconductor solutions and their challenges, EEMODS 2016, Helsinki
- [6] C. R. Müller, et al., New 1200 V IGBT and Diode Technology with Improved Controllability for Superior Performance in Drives Application, PCIM Europe, Nuremberg, Germany, 2018
- [7] C. Jaeger, et al., A New Sub-Micron Trench Cell Concept in Ultrathin. Wafer Technology for Next Generation 1200 V IGBTs, ISPSD, Sapporo, Japan, 2017
- [8] K. Vogel, et al., IGBT inverter with increased power density by use of high-temperature-capable and low-inductance design, PCIM Europe, Nuremberg, Germany, 2012
- [9] AN2018-14, TRENCHSTOP™ 1200 V IGBT7 Application Note,
https://www.infineon.com/dgdl/Infineon-AN_201814_TRENCHSTOP_1200V_IGBT7-AN-v01_00-EN.pdf?fileId=5546d46265487f7b01656b173ddc3600